JOC The Journal of Organic Chemistry

Article

pubs.acs.org/joc

Charge Transfer Emission in Oligotriarylamine–Triarylborane Compounds

Annabell G. Bonn and Oliver S. Wenger*

Department of Chemistry, University of Basel, St. Johanns-Ring 19, CH-4056 Basel, Switzerland

Supporting Information

ABSTRACT: Donor–acceptor compounds exhibiting charge transfer emission are of interest in a variety of different contexts, for example, for nonlinear optical processes and for sensor applications. Recently investigated triarylamine–triarylborane compounds represent an important class of donor–acceptor systems, and we explored to what extent their charge-transfer properties can be further improved by using stronger amine donors and borane acceptors than prior studies. The oligotriarylamine employed here is a much stronger donor than previously used triarylamines containing single nitrogen centers. In order to increase the acceptor strength, the electron-accepting unit was equipped with two (instead of one) dimesitylboron substituents. In our comparative study, six donor–acceptor compounds were synthesized and investigated by cyclic voltammetry and optical spectroscopy. An increase of the donor strength through replacement of an ordinary triarylamine by an oligotriarylamine unit leads to the expected energetic stabilization of charge transfer (CT) excited states, but the emission solvatochromism is not more pronounced. The attempted increase of the acceptor strength by substitution of the acceptor moiety by two (instead of one) dimesitylboron groups leads to a drastic decrease of emission quantum yields. On the basis of these results, our purely experimental study provides fundamental guidelines for the design of new triarylamine–triarylborane donor–acceptor compounds with favorable charge-transfer emission properties.

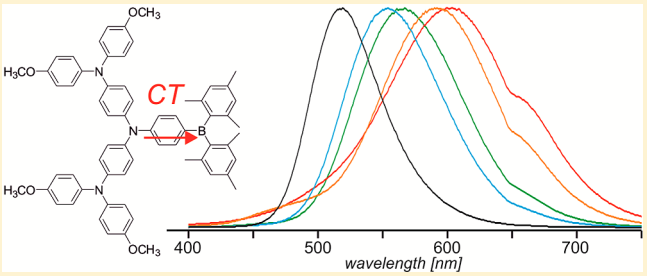

INTRODUCTION

Donor–acceptor compounds have fascinated chemists for many decades, but research on such molecules remains an important topic even nowadays because donor–acceptor compounds find application in many different areas. For example, many recently developed organic dyes for solar cells are donor–acceptor compounds.[1] For imaging, luminescent donor–acceptor compounds are of great current interest, because two-photon absorption followed by charge transfer emission can be used to convert two near-infrared input photons into one visible output photon.[2] Other donor–acceptor compounds are explored in the context of sensor materials, or, when part of conjugated oligomers or polymers, for light-emitting diodes and charge transfer networks in general.[2b,3] For fundamental studies, investigation of discrete donor–acceptor molecules in solution with UV–vis absorption, photoluminescence, and cyclic voltammetry remains a valuable experimental approach.

4-(Dimethylamino)benzonitrile (DMABN) and its derivatives are among the best known examples of donor–acceptor compounds,[4] but in recent years, attention has shifted to other types of systems. An important class of relatively new donor–acceptor compounds is comprised of triarylamine donor and triarylborane acceptor moieties, linked together covalently via π-conjugated molecular bridges.[5] Some of these triarylamine–triarylborane systems have been employed as molecular sensors which are selective for fluoride and cyanide;[6] the detection process is often based on a change in optical absorption or emission due to a shift of charge transfer (CT) states upon anion binding at the triarylborane.[6e,7] In other cases, the motivation for study of triarylamine–triarylborane compounds came from the interest in new luminescent materials or from a fundamental interest in the CT process.[8] Compounds with multiple arylamine donor/arylborane acceptor sites have also been explored.[9]

The aim of this project was to explore whether the favorable CT properties of triarylamine–triarylborane compounds could be further improved by making the donor and acceptor groups even stronger while keeping the donor–acceptor distance relatively short. Toward this end, we performed a comparative study of the CT behavior of "traditional" triarylamine–triarylborane compounds (N-ph-B, N-phCC-B; Scheme 1a) and two molecules with an oligotriarylamine donor and a triarylborane acceptor (N_3-ph-B, N_3-phCC-B; Scheme 1b). The oligotriarylamine is known to have significantly lower oxidation potentials than ordinary triarylamines;[10] i.e., it is a substantially stronger electron donor than ordinary triarylamines with single N centers. In an attempt to probe the additional effect resulting from an increase of acceptor strength, two compounds equipped with two dimesitylboron centers (N_3-ph-B_2, N_3-phCC-B_2; Scheme 1c) were investigated. The rationale for this

Received: February 23, 2015
Published: April 3, 2015

DOI: 10.1021/acs.joc.5b00416
J. Org. Chem. 2015, 80, 4097–4107

Scheme 1. Molecular Structures of the Donor–Acceptor Compounds Investigated in This Work

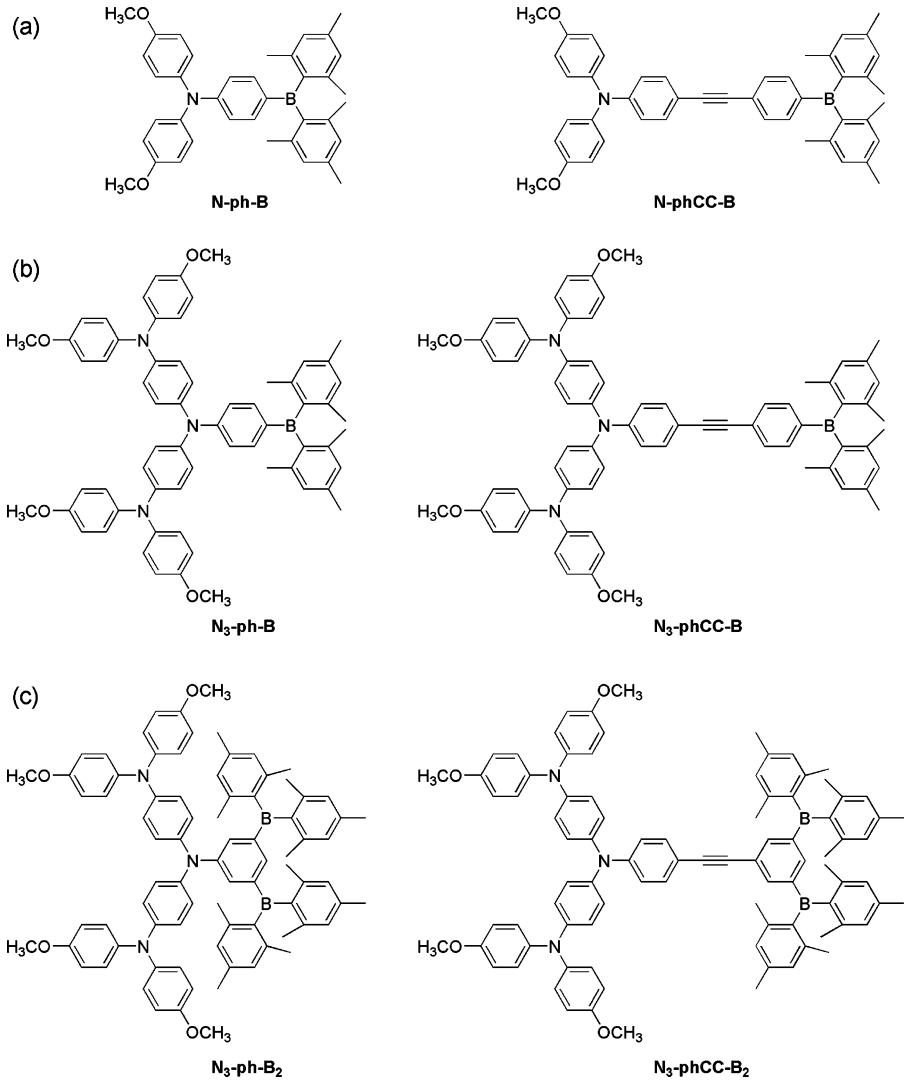

acceptor design is that the presence of two electron-deficient boron substituents will increase the reduction potential of the acceptor, i.e., make it easier to reduce. This, however, necessitates attachment of the boron atoms in the *meta*-position to the amine donor.

Our study is of purely experimental nature, as the purpose of this work was to establish guiding principles for the molecular design of new triarylamine–triarylborane donor–acceptor compounds with favorable CT emission properties, based on phenomenological observations.

RESULTS AND DISCUSSION

Synthesis. The acceptor moieties were synthesized by reacting 1,4-dibromobenzenze (**1**) or 1,3,5-tribromobenzene (**4**) with dimesitylboron fluoride (**2**), yielding compounds **3**,[11] **5**,[12] and **6** (Scheme 2).[13] **3** and **6** were coupled to dianisylamine (**7**) or an equivalent oligotriarylamine building block (**8**)[10c] to afford N-ph-B, N_3-ph-B, and N_3-ph-B_2. For the second series of donor–acceptor compounds, the starting point was 4-bromo-1-iodobenzene (**9**) which was coupled to trimethylsilyl acetylene (**10**) to result in compound **11** (Scheme 3).[14] The latter was reacted with the above-mentioned amines **7** or **8** in Pd-catalyzed N–C coupling reactions, yielding compounds **12** and **13**.[15] Deprotection of the trimethylsilyl groups resulted in the acetylene compounds **14** and **15** which were reacted with the borane building blocks **3** or **6** to afford N-phCC-B,[9b] N_3-phCC-B, and N_3-phCC-B_2.

Electrochemistry. Cyclic voltammetry was used to measure the electrochemical potentials for donor oxidation and acceptor reduction in the six compounds from Scheme 1. In Figure 1, the voltammograms for N-ph-B, N_3-ph-B, and N_3-ph-B_2 measured in dry and deoxygenated THF at 25 °C in the presence of 0.1 M $TBAPF_6$ are shown. Oxidation of the triarylamine moiety of N-ph-B (Figure 1a) occurs at 0.33 V vs Fc^+/Fc, while reduction of the triarylborane unit takes place at −2.75 V vs Fc^+/Fc (Table 1). Both potentials are in line with previously reported values for comparable compounds.[16] Oxidation of the oligotriarylamine donor in N_3-ph-B to its monocationic form occurs at −0.02 V vs Fc^+/Fc (Figure 1b), and the dication is formed at 0.15 V vs Fc^+/Fc. At higher potentials, oxidation of the third N center is commonly observed in oligotriarylamines,[10] but this is often an irreversible process, and it occurs outside the potential window considered in Figure 1. For the CT emission properties of our donor–acceptor compounds, only oxidation of the first N center is relevant because the lowest-energy CT state involves only the

DOI: 10.1021/acs.joc.5b00416
J. Org. Chem. 2015, 80, 4097–4107

Scheme 2. Synthesis of Donor–Acceptor Compounds[a]

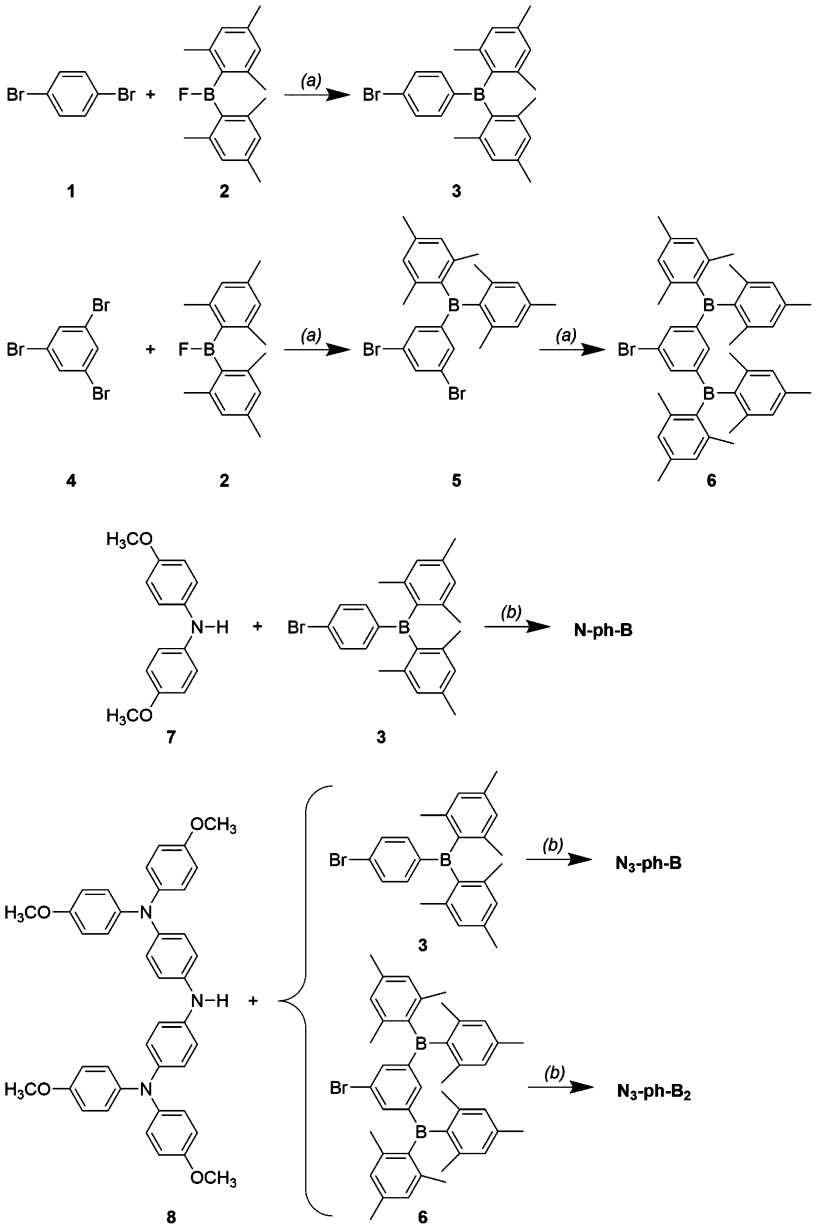

[a](a) *n*-BuLi, Et_2O, −78 °C; (b) $Pd(dba)_2$, NaO^{t}Bu, $(HP^tBu_3)BF_4$, toluene, reflux. For single reaction steps, the yields of the individual compounds were the following: **3**, 80%; **5**, 69%; **6**, 69%; N-ph-B, 92%; N_3-ph-B, 77%; N_3-ph-B_2, 63%.

electron in the energetically highest orbital. This first oxidation occurs at the central N atom of the oligotriarylamine because this is the most electron-rich position.[10a] CT excitations at higher energies may of course involve the peripheral, less readily oxidizable N atoms, but these states are not emissive. From the data in Figure 1 and Table 1, we conclude that oligotriarylamine is a stronger one-electron donor than the ordinary triarylamine by ∼0.35 eV. This is markedly different from what can be achieved in simple NAr_2 donors (Ar = C_6H_4R; R = H, OMe, etc.); in this regard, the oligotriarylamine used here is special.

The triarylborane reduction potential is only marginally affected by the change in amine between N-ph-B and N_3-ph-B (Table 1). However, when the acceptor moiety is equipped with two boron centers (N_3-ph-B_2), its reduction potential shifts to less negative values by about 0.2 V (Figure 1c, Table 1). Intuitively, this makes sense because two electron-withdrawing dimesitylboron groups will lead to a less electron-rich compound than only one dimesitylboron substituent. On the other hand, in N_3-ph-B_2, the dimesitylboron groups are electronically more decoupled from the amino unit than in N-ph-B or in N_3-ph-B because the respective electro-active groups are in the *meta*- rather than *para*-position to each other. Donation of electron density from the amino groups toward the boron atoms is therefore expected to be weaker in N_3-ph-B_2 than in N-ph-B and in N_3-ph-B, and this could also lead to a shift of the dimesitylboron-related reduction potential to less negative values. It is not a priori clear which one of these two effects has a dominant influence or whether they both contribute to similar extents. Obviously, a reference molecule equipped with only one dimesitylboron substituent in the *meta*-position to the amino group would be

DOI: 10.1021/acs.joc.5b00416
J. Org. Chem. 2015, 80, 4097–4107

Scheme 3. Synthesis of Donor–Acceptor Compounds[a]

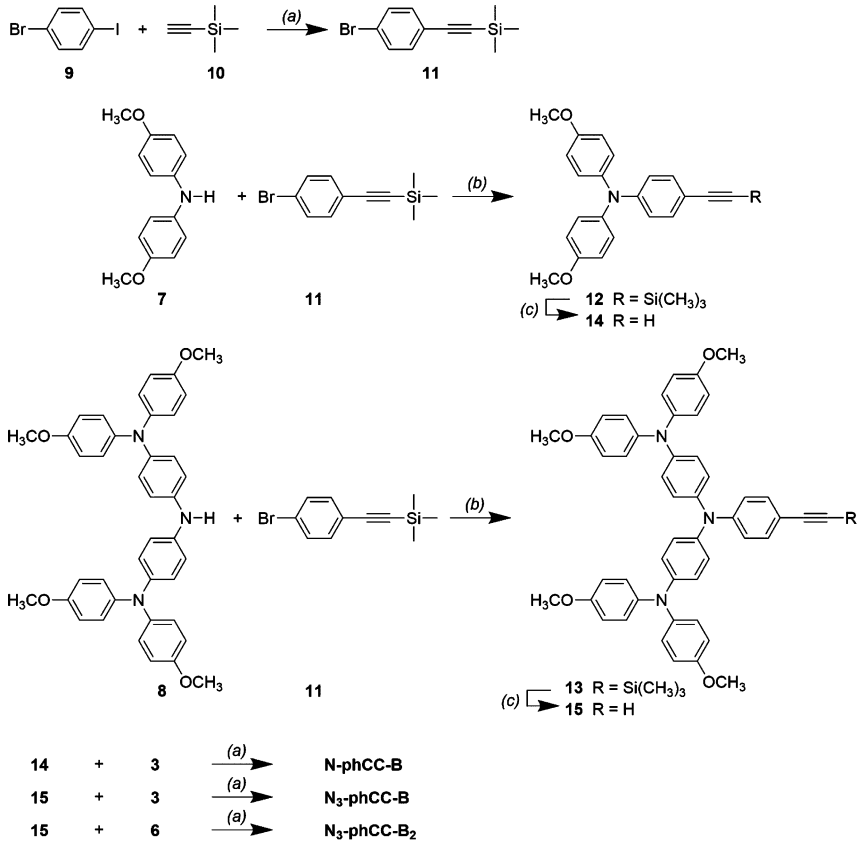

[a](a) $PdCl_2(PPh_3)_2$, CuI, Et_3N, reflux; (b) $Pd(dba)_2$, NaO^tBu, $(HP^tBu_3)BF_4$, toluene, reflux; (c) TBAF, THF, 25 °C. For single reaction steps, the yields of the individual compounds were the following: **11**, ~100%; **12**, 64%; **13**, 74%; **14**, 99%; **15**, 91%; N-phCC-B, 43%; N_3-phCC-B, 42%; N_3-phCC-B_2, 34%.

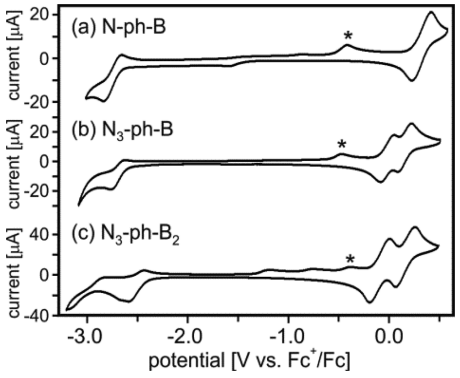

Figure 1. Cyclic voltammograms measured for (a) N-ph-B, (b) N_3-ph-B, and (c) N_3-ph-B_2 in dry and deoxygenated THF with 0.1 M $TBAPF_6$. The potential sweep rate was 0.1 V/s in all cases. The waves marked with an asterisk (*) were only detected after an initial oxidative sweep to potentials more positive than 0.5 V vs Fc^+/Fc and are attributed to electrochemical side products.

useful to address this question, but this is beyond the scope of the present study. For our purposes, it is sufficient to note that reduction of N_3-ph-B_2 occurs more easily by ca. 0.2 V than reduction of N-ph-B and N_3-ph-B.

Regarding donor oxidation, completely analogous observations are made for the series of compounds containing additional ethynyl spacers (N-phCC-B, N_3-phCC-B, N_3-phCC-B_2); the respective voltammograms are shown in Figure S1 (Supporting Information). Triarylborane reduction is easier by ~0.4 V in N-phCC-B and N_3-phCC-B compared to their analogues without ethynyl spacers (N-ph-B, N_3-ph-B). Attachment of a second boron center to the acceptor site (in compound N_3-phCC-B_2) does not result in a further increase of the reduction potential.

For each compound, the free energy for electron transfer (ΔG_{CT}^0) from the amine donor to the borane acceptor can be estimated using the relation $\Delta G_{CT}^0 \approx e[E(\text{amine}^{+/0}) - E(\text{borane}^{0/-})]$, leading to the values in the fifth column of Table 1 (e is the elemental charge). The respective free energies do not directly correspond to the expected optical CT energies (E_{CT}) because the latter involve Franck–Condon transitions between excited states and vibrationally unrelaxed ground states (in emission). However, within a homologous series of compounds, the estimated ΔG_{CT}^0 values should at least reflect the trends in optical CT energies. Inspection of Table 1 shows that this is indeed the case. The E_{CT} values in Table 1 were derived from emission band maxima. A more correct treatment would be based on the energies of the electronic origins of the CT absorption and emission bands (E_{00}), but from room-temperature solution spectra, the respective energies can only be determined with large uncertainties. In the last column of Table 1, we report E_{00} values estimated on the basis of emission band onsets. Expectedly, E_{00} and E_{CT} follow the same trend because the excited-state distortions are similar in all compounds considered here, and consequently, the correlation

DOI: 10.1021/acs.joc.5b00416
J. Org. Chem. 2015, 80, 4097–4107

Table 1. Electrochemical Potentials (in Volts vs Fc^+/Fc) for Oxidation of Amine-Based Donor Moieties and for Reduction of Triarylborane-Based Acceptor Moieties in the Compounds from Scheme 1 in THF[a]

	$E(\text{amine}^{+/0})$	$E(\text{amine}^{2+/+})$	$E(\text{borane}^{0/-})$	$\Delta G_{CT}{}^{0\,b}$ (eV)	$E_{CT}{}^{c}$ (eV)	$E_{00}{}^{d}$ (eV)
N-ph-B	0.33		−2.75	3.08	2.73	3.05
N_3-ph-B	−0.02	0.15	−2.69	2.67	2.39	2.74
N_3-ph-B_2	−0.09	0.17	−2.52	2.43	2.11	2.64
N-phCC-B	0.29		−2.37	2.66	2.80	3.03
N_3-phCC-B	−0.06	0.12	−2.36	2.30	2.44	2.82
N_3-phCC-B_2	−0.06	0.16	−2.48	2.42	2.68	2.98

[a]Extracted from the data in Figure 1 and Figure S1 (Supporting Information); measured in the presence of 0.1 M $TBAPF_6$, using dry and deoxygenated solvent and potential sweep rates of 0.1 V/s. [b]$\Delta G_{CT}{}^0$ is the free energy for electron transfer from amine to borane calculated as $\Delta G_{CT}{}^0 \approx e[E(\text{amine}^{+/0}) - E(\text{borane}^{-/0})]$. This free energy may be regarded as a measure for the energy of the optical N → B charge transfer; see text. [c]E_{CT} is the energetic position of the CT emission band maximum in hexane. [d]E_{00} is the energy of the electronic origin of the emissive CT state, estimated from the emission onsets.

between $\Delta G_{CT}{}^0$ and E_{00} is equally as good as the correlation between $\Delta G_{CT}{}^0$ and E_{CT} within a given series of compounds.

Optical Absorption and Emission Spectroscopy in Hexane. In Figure 2 the UV−vis absorption (solid lines) and luminescence spectra (dotted lines) of (a) N-ph-B, (b) N_3-ph-B, and (c) N_3-ph-B_2 in hexane at 25 °C are shown. Under these conditions, the lowest-energy absorption band maxima are at 383 nm for N-ph-B and at 410 nm for N_3-ph-B, and these bands are attributed to CT transitions. In the spectrum of N_3-ph-B_2, there is an intense band with a maximum at 321 nm, but this is not the lowest-energy absorption. The intense band at 321 nm is attributed to a $\pi-\pi^*$ transition, while the CT transition is merely observable as a shoulder between 400 and 550 nm (Figure S2, Supporting Information).

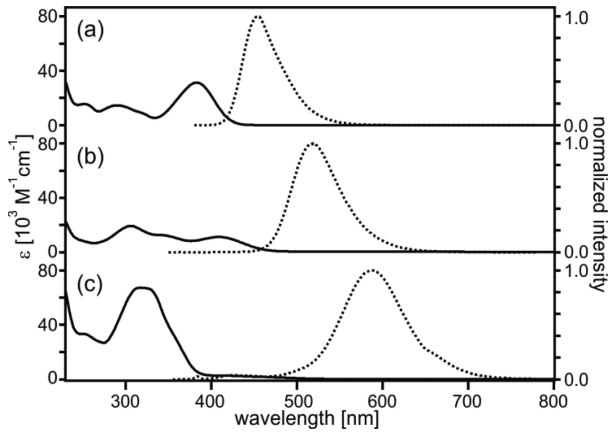

Figure 2. UV−vis absorption (solid lines) and normalized luminescence spectra (dotted lines) of (a) N-ph-B (λ_{exc} = 370 nm), (b) N_3-ph-B (λ_{exc} = 330 nm), and (c) N_3-ph-B_2 (λ_{exc} = 345 nm) in hexane at 25 °C. (λ_{exc} denotes the excitation wavelength.)

In the case of N_3-ph-B_2, CT absorption is comparatively weak due to poor electronic coupling between the amine donor and the dimesitylboron substituents which are connected to the bridging phenylene unit in the *meta*- rather than *para*-position. The oscillator strength is proportional to the squared electronic coupling matrix element; hence, even a relatively small decrease in donor−acceptor coupling strength can entail a substantial decrease in oscillator strength. It is well-known that electronic couplings between *meta*-substituents at phenylene bridging units are significantly weaker than electronic couplings between *para*-substituents. In this regard, our finding of weak CT absorption in N_3-ph-B_2 is not at all surprising; the rationale for this *meta*-substitution pattern is described in the Introduction.

The emission band maxima of N-ph-B, N_3-ph-B, and N_3-ph-B_2 in hexane at 25 °C occur at 454, 518, and 587 nm and thus follow the trend predicted for CT energies based on the electrochemical data (fifth column of Table 1).

For the series of compounds with additional ethynyl linkers (right part of Scheme 1), similar absorption and emission behavior is observed. The key difference is that the CT emission maxima follow a different trend than that for the compounds without ethynyl linkers (Figure S3, Supporting Information), increasing in wavelength from 443 to 508 nm between N-phCC-B and N_3-phCC-B but then decreasing to 462 nm for N_3-phCC-B_2. However, this trend follows exactly the prediction made on the basis of the electrochemical data (last two columns of Table 1).

Solvatochromism and Changes in Dipole Moment. In Figure 3a, the CT emission of N-ph-B in five different solvents at 25 °C is shown. The focus was set on hexane, toluene, diethyl ether, THF, and CH_2Cl_2 for all six compounds from Scheme 1, because in these solvents luminescence quantum yields are above 3% in most cases. Solvents of higher polarity (e.g., acetone, DMF, DMSO) lead to lower luminescence quantum yields, and it becomes difficult to distinguish between luminescence emitted by the compounds under study and

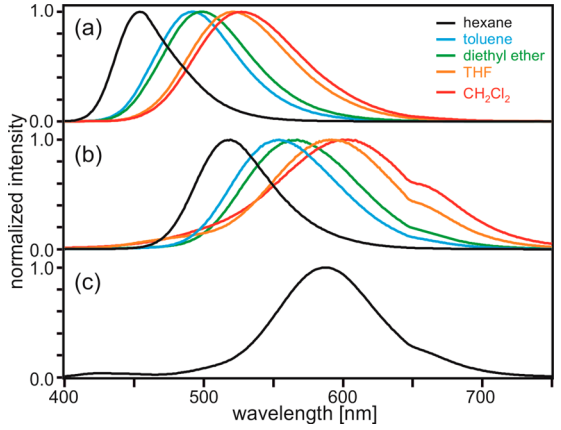

Figure 3. Normalized photoluminescence of (a) N-ph-B, (b) N_3-ph-B, and (c) N_3-ph-B_2 in various solvents at 25 °C. Excitation wavelengths (λ_{exc}) were as follows: 370 nm for N-ph-B, 330 nm for N_3-ph-B, and 345 nm for N_3-ph-B_2. The kink at 650 nm in the spectra from panels b and c is an artifact caused by the instrument.

DOI: 10.1021/acs.joc.5b00416
J. Org. Chem. 2015, 80, 4097−4107

artifacts. As the solvent polarity increases, there is a pronounced red-shift of the emission, as expected for this class of compounds.[8c,17] For N-ph-B, the solvatochromic shift of the band maximum amounts to 3050 cm^{-1} between hexane and CH_2Cl_2 (Figure 3a), and for N_3-ph-B, it is 2720 cm^{-1} (Figure 3b). The N_3-ph-B_2 compound only emits significantly in hexane (Figure 3c). Positive solvatochromism is also observed for the emission of N-phCC-B, N_3-phCC-B, and N_3-phCC-B_2 (Figure S4, Supporting Information). The latter two compounds only emit significantly in hexane, toluene, and diethyl ether; hence, the shift in emission band maxima between hexane and diethyl ether is a useful measure for comparison of solvatochromism in the molecules from the right half of Scheme 1. For N-phCC-B, the respective shift is 3000 cm^{-1}, for N_3-phCC-B it is 2760 cm^{-1}, and for N_3-phCC-B_2 we detect 3720 cm^{-1}. With the exception of N_3-phCC-B_2, emission solvatochromism is not more pronounced in the oligotriarylamine–triarylborane compounds than in the reference molecules containing ordinary triarylamine donors with single nitrogen centers (N-ph-B, N-phCC-B).

In optical absorption spectroscopy, hardly any solvatochromism is detected for all compounds from Scheme 1 (Figures S5 and S6, Supporting Information). This is not unexpected because the electronic ground state is associated with a substantially weaker dipole moment than the CT excited state.[8g,17a] In Figure 4, the CT absorption and emission band maxima of N-ph-B and N_3-ph-B are plotted as a function of solvent polarity (expressed in the form of Reichhardt parameters);[18] analogous plots for N-phCC-B, N_3-phCC-B, and N_3-phCC-B_2 are shown in Figure S7 (Supporting Information). It is evident from these plots that solvatochromism is far more pronounced in emission than in absorption.

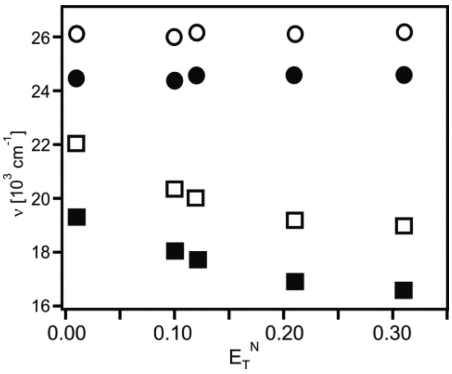

Figure 4. Absorption (circles) and emission band maxima (squares) as a function of solvent polarity (expressed in the form of Reichhardt parameters).[18] Open circles and squares, N-ph-B; filled circles and squares, N_3-ph-B.

As an alternative to the Reichhardt parameter plots, the method by Lippert and Mataga is frequently employed for analysis of the solvent dependence of absorption and emission bands.[19] This method permits estimation of the difference between ground- and excited-state dipole moments ($\Delta\mu_{eg}$) from the dependence of the Stokes shift on solvent polarity (eq 1).

$$hc(\upsilon_{abs} - \upsilon_{em}) = hc(\upsilon_{abs}^{vac} - \upsilon_{em}^{vac})\frac{2(\Delta\mu_{eg})^2}{a_0^3}\left[\frac{\varepsilon - 1}{2\varepsilon + 1} - \frac{\eta^2 - 1}{2\eta^2 + 1}\right] \quad (1)$$

In eq 1, the solvent polarity is captured by the $(\varepsilon - 1)/(2\varepsilon + 1) - (\eta^2 - 1)/(2\eta^2 + 1)$ term in which ε is the dielectric constant and η is the refractive index.[19] The $hc(\nu_{abs} - \nu_{em})$ and $hc(\nu_{abs}^{vac} - \nu_{em}^{vac})$ terms are the differences in absorption and emission maxima in a given solvent and in a vacuum, respectively. In our cases, these are simply the Stokes shifts for the CT transition in a given solvent and in a vacuum, and $hc(\nu_{abs} - \nu_{em})$ can readily be determined from our experimental data in Figure 3 and Figures S4, S5, and S6 (Supporting Information). In Figure 5, we show plots of $hc(\nu_{abs} - \nu_{em})$ versus $(\varepsilon - 1)/(2\varepsilon + 1) - (\eta^2 - 1)/(2\eta^2 + 1)$ for N-ph-B (a) and N_3-ph-B (b). Linear regression fits yield $hc(\nu_{abs}^{vac} - \nu_{em}^{vac})$ from the intercept and $2\Delta\mu_{eg}^2/a_0^3$ from the slope; the parameter a_0 is the so-called Onsager radius of the solvent cavity formed around the chromophore.[20] The key outcome from this analysis is that the slope (i.e., the ratio of $2\Delta\mu_{eg}^2$ and a_0^3) is within experimental accuracy the same for N-ph-B (10500 ± 3000 cm^{-1}) and N_3-ph-B (10000 ± 2300 cm^{-1}). Estimation of the Onsager radius is usually associated with significant uncertainty, and even small errors in a_0 will have a large impact on the estimated value for $\Delta\mu_{eg}$ when attempting to extract dipole moment changes from $2\Delta\mu_{eg}^2/a_0^3$ ratios.[17a,21] Furthermore, it is usually debatable to what extent the solvent cavity can indeed be approximated as spherical. In view of these limitations and the relatively modest linear correlations found

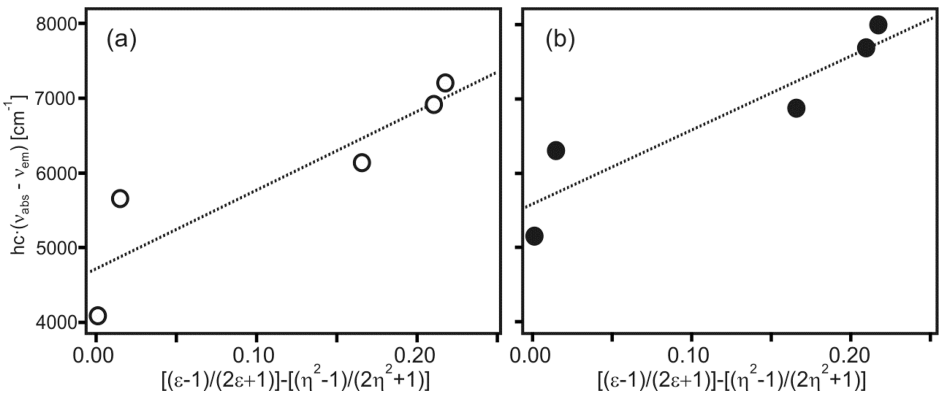

Figure 5. Lippert–Mataga plot showing the dependence of Stokes shift between CT absorption and emission on solvent polarity for (a) N-ph-B and (b) N_3-ph-B.

DOI: 10.1021/acs.joc.5b00416
J. Org. Chem. 2015, 80, 4097–4107

Scheme 4. Illustration of Ground- and Excited-State Dipole Moments (Arrows in the Centers) in N_3-ph-B (Left) and N-ph-B (Right) and Solvent Dipole Moments (Elliptical Objects) with Onsager Radii (a_0; Dotted Circles)

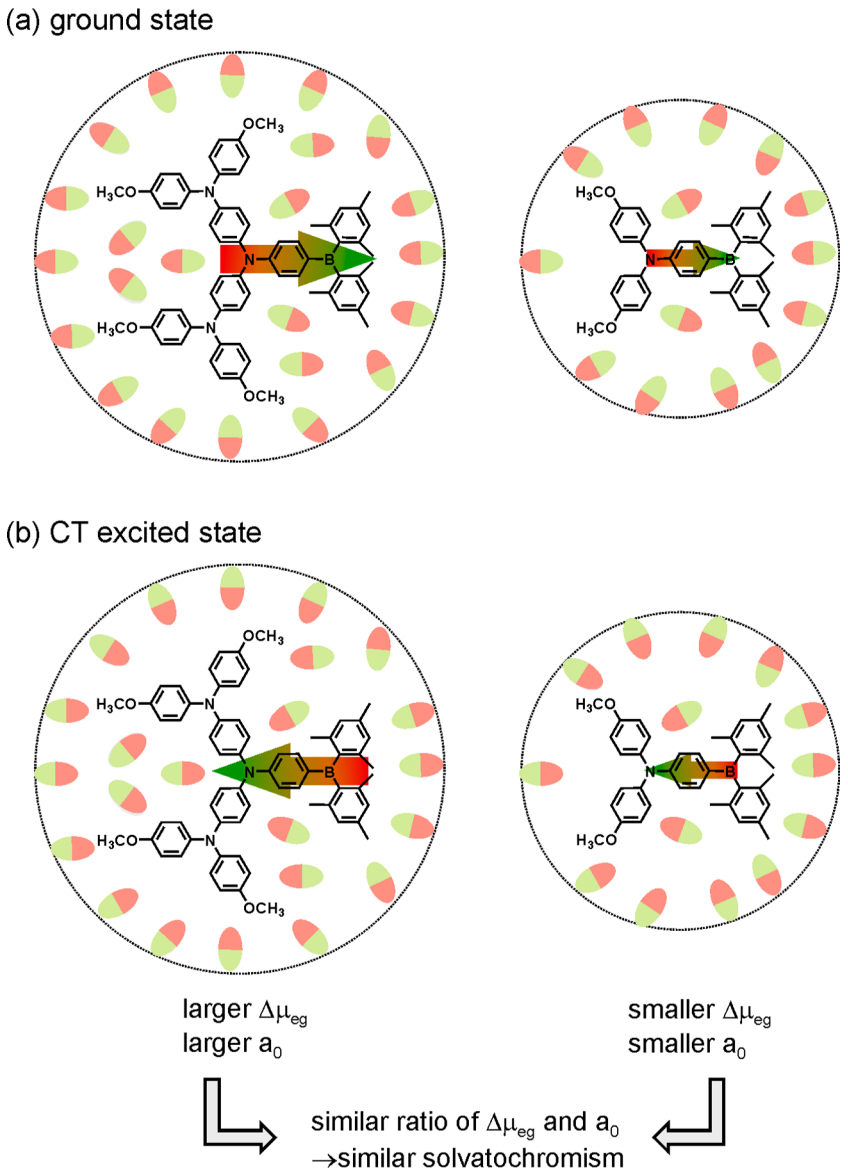

Table 2. Luminescence Quantum Yields (ϕ) and Lifetimes (τ) in Aerated Solvents at 25 °C

	hexane		toluene		diethyl ether		THF		CH_2Cl_2	
cmpd	ϕ	τ (ns)	ϕ	τ (ns)	ϕ	τ (ns)	ϕ	τ (ns)	ϕ	τ (ns)
N-ph-B	0.59	4.1	0.72	6.0	0.75	7.4	0.63	7.6	0.66	8.6
N_3-ph-B	0.49	5.8	0.50	7.8	0.40	7.0	0.12	2.7	0.04	1.1
N_3-ph-B_2	0.06	11.8								
N-phCC-B	0.81	1.8	0.85	2.6	0.88	3.6	0.49	2.8	0.38	2.4
N_3-phCC-B	0.63	3.6	0.52	4.1	0.11	1.8				
N_3-phCC-B_2	0.21	3.8	0.13	9.3	0.08	13.2				

in Figure 5 (R^2 = 0.81 and 0.86, respectively), it seems appropriate to simply make the following semiquantitative point: When going from N-ph-B to N_3-ph-B, the increase in molecular size may well be associated with a 25% increase in Onsager radius. Such a relatively modest increase in a_0 can completely mask a 40% increase in $\Delta\mu_{eg}$. In other words, CT in N_3-ph-B is indeed likely to be associated with a significantly increased change in dipole moment when compared to N-ph-B. However, this anticipated and desired effect is outbalanced by the increase in Onsager radius, and the net result is similar solvatochromism in N_3-ph-B and N-ph-B. This key outcome is graphically summarized in Scheme 4. Keeping the molecular size small while increasing the push−pull character is therefore an important guiding principle for the design of future triarylamine−triarylborane compounds, at least when aiming at strong solvatochromism.

DOI: 10.1021/acs.joc.5b00416
J. Org. Chem. 2015, 80, 4097−4107

Luminescence Quantum Yields and Lifetimes. The luminescence quantum yields of the individual donor−acceptor compounds from Scheme 1 correlate reasonably well with the energetic position of the emission band maximum (Table 2). As the CT excited state shifts to lower energies, luminescence quantum yields tend to decrease. This behavior is compatible with the so-called energy gap law which states that nonradiative relaxation processes become increasingly efficient with decreasing energy gap between emissive excited state and ground state (or energetically next lower-lying excited state).[22] However, there is no clear correlation between quantum yields and excited state lifetimes, suggesting that both radiative and nonradiative excited-state decay rates vary substantially from one solvent to the other. The efficiency of nonradiative relaxation processes is notoriously difficult to rationalize, but one possibility is that interactions between solvent donor molecules and the dimesitylboron acceptor groups provide an efficient thermal relaxation pathway. This effect could become increasingly efficient with increasing solvent polarity. On the other hand, the boron center is relatively well shielded from its chemical environment due to the bulky mesityl substituents.

While N-ph-B, N_3-ph-B, and N-phCC-B exhibit strong CT emission in all five solvents considered here, the doubly dimesitylboron-substituted compounds N_3-ph-B_2 and N_3-phCC-B_2 exhibit poor luminescence properties. Two-fold boron substitution of the acceptor group was motivated by an increase in acceptor strength, but this requires attachment of the dimesitylboron groups in the *meta*-position relative to the N donor atom. As noted above, this entails a substantial decrease of the oscillator strength associated with CT absorption in N_3-ph-B_2 and N_3-phCC-B_2 compared to the other compounds from Scheme 1 in which N and B atoms are in the *para*-position relative to each other. This effect has implications for the emission behavior of N_3-ph-B_2 and N_3-phCC-B_2 because radiative decay rate constants are proportional to oscillator strengths. Thus, because of their weaker donor−acceptor coupling caused by the *meta*-linkage, N_3-ph-B_2 and N_3-phCC-B_2 not only exhibit weaker CT absorption but they also have lower radiative decay rate constants from the CT state. Moreover, if interaction between solvent donor molecules and the dimesitylboron acceptor groups indeed provide an efficient thermal relaxation pathway as suspected above, then one might argue that this effect is amplified in the presence of two (instead of one) acceptor groups. Consequently, there are two effects that both can contribute to the low luminescence quantum yields of N_3-ph-B_2 and N_3-phCC-B_2: (i) a decrease of radiative excited-state decay rate constants and (ii) an increase of nonradiative excited-state decay rate constants.

Another noteworthy observation from Table 2 is that luminescence quantum yields are lower in N_3-ph-B than in N-ph-B (and similarly in N_3-phCC-B compared to N-phCC-B). Thus, the use of an oligotriarylamine donor in place of a simple triarylamine has a negative influence on the luminescence properties, particularly with increasing solvent polarity. The oscillator strengths for CT absorptions are similar in these four compounds in all five solvents considered here (Figures S5 and S6, Supporting Information); hence, there is no physical basis for assuming that the radiative decay rate constants for CT emission would be much different between these compounds in this range of solvents. Consequently, the observed differences in quantum yields are most likely due to differences in nonradiative excited-state relaxation. Two aspects seem important in this regard: (i) oligotriarylamines are made of more atoms than simple triarylamines, and hence, the number of vibrational degrees of freedom is greater in N_3-ph-B and N_3-phCC-B than in N-ph-B and N-phCC-B; (ii) the CT states are ∼0.4 eV lower in energy in N_3-ph-B and N_3-phCC-B compared to N-ph-B and N-phCC-B (Table 1). Lower luminescence quantum yields in the oligotriarylamine systems are therefore in line with the energy gap law. As the emissive CT state is energetically further stabilized by increasing solvent polarity, multiphonon relaxation becomes increasingly efficient, and this effect is particularly dramatic for N_3-ph-B and N_3-phCC-B because in these cases the CT energy in the more polar solvents approaches only 5−6 quanta of C−H stretching vibrations. At least in so-called "weak coupling" cases (i.e., in systems in which there are only small distortions between ground and excited states), this is typically the limit when multiphonon relaxation begins to dominate. It is commonly the highest-frequency vibration of a molecular system which is relevant because this is the most efficient promoter of energy dissipation, hence our reference to C−H stretching vibrations. Thus, the lower luminescence quantum yields of N_3-ph-B and N_3-phCC-B with respect to N-ph-B and N-phCC-B can be understood on relatively simple grounds.

Finally, we note that the N-phCC-B and N_3-phCC-B compounds have slightly higher luminescence quantum yields than N-ph-B and N_3-ph-B; i.e., introduction of the ethynyl linker has a mildly beneficial influence on the luminescence properties but only in the most apolar solvents hexane and toluene (and diethyl ether in the case of N-phCC-B/N-ph-B). This is a comparatively subtle effect which most likely has its origin in different nonradiative excited-state relaxation rates; the relevant CT absorptions have similar oscillator strengths regardless of whether ethynyl linkers are present or not (Figures S5 and S6, Supporting Information); hence, the radiative excited-state decay rates are likely to be largely unaffected by this change of linker. As a guiding principle for the molecular design of new emissive triarylamine−triarylborane compounds, it can be stated that ethynyl linkers have a mildly beneficial influence on luminescence quantum yields in strongly apolar solvents but they become detrimental in even very weakly polar solvents such as THF and CH_2Cl_2. Clearly, the influence of the ethynyl linker on luminescence quantum yields is weak compared to the influence of 2-fold dimesitylboron substitution and replacement of ordinary triarylamine by oligotriarylamine (see above).

■ SUMMARY AND CONCLUSIONS

The aim of this study was to explore the potential for improvement of CT emission properties of triarylamine−triarylborane donor−acceptor compounds from a purely experimental point of view and to establish guiding principles for the molecular design of new systems of this type. All key observations and trends observed for the six compounds from Scheme 1 can be adequately rationalized on the basis of simple physicochemical principles. The key findings from this study are the following:

(i) Trends in CT energies of unknown triarylamine−triarylborane compounds can be predicted on the basis of electrochemical potentials of the individual donor and acceptor components.

(ii) Oligotriarylamines lead to the expected red-shift of CT emission because they are substantially stronger donors than simple triarylamines, but the increase in molecular

DOI: 10.1021/acs.joc.5b00416
J. Org. Chem. 2015, 80, 4097−4107

size entails a larger solvent cavity; i.e., more solvent dipole moments oppose the dipole moment change associated with CT in the donor−acceptor molecule. The net result is a solvatochromic effect of similar magnitude as with ordinary triarylamines because the increase in dipole moment change upon CT excitation is compensated by an increase in Onsager radius.

(iii) The attempted increase of acceptor strength by 2-fold dimesitylboron substitution is a failure in several regards. First, the effect on the acceptor reduction potential is relatively small. Second, 2-fold substitution forcedly occurs in the *meta*-position to the amine donor, and this lowers the oscillator strength of the CT absorption considerably due to weaker electronic coupling between the donor and the acceptor, and more importantly, it lowers radiative decay rate constants from the CT excited states. Low CT luminescence quantum yields result.

(iv) Luminescence quantum yields with oligotriarylamine donors are somewhat lower than with simple triarylamines due to more efficient multiphonon relaxation processes.

From these key findings, the following guiding principles for the design of future systems with amine donor and borane acceptor groups emerge:

(i) Size matters: When modifying the donor and/or acceptor groups in an attempt to enhance the CT properties, it is desirable to keep the overall molecular size as small as possible.

(ii) The radiative decay rate for the CT excited state must be kept large by providing strong electronic coupling between the donor and acceptor groups. *p*-Phenylene and *p*-phenylene ethynylene linkers behave similarly in this regard.

(iii) Very electron-rich triarylamines which are smaller than the oligotriarylamine used here would be desirable.

(iv) An increase in acceptor strength is better performed by fluorination of dimesitylboron units than by increasing the number of dimesitylboron substituents.[23]

EXPERIMENTAL SECTION

Compound **3**.[11] 1,4-Dibromobenzene (**1**) (1.75 g, 7.42 mmol) was dissolved in dry Et_2O (20 mL) under N_2. After cooling to −78 °C, *n*-BuLi in hexane was added dropwise (3.40 mL, 5.44 mmol), and the mixture was stirred at this temperature for 3 h. A solution of dimesitylboron fluoride (**2**) (1.56 g, 5.82 mmol) in dry Et_2O was added dropwise, and the suspension was stirred at room temperature overnight. Et_2O (50 mL) was added, and the organic phase was washed with saturated aqueous NH_4Cl solution (100 mL) and with water. After drying over anhydrous Na_2SO_4 and subsequent evaporation of the solvent, the raw product was purified by column chromatography on silica gel using pentane as the eluent. The pure product was obtained as a white solid (2.49 g, 6.15 mmol, 80%). ^{1}H NMR (400 MHz, $CDCl_3$): δ [ppm] 7.43 (ABq, 4 H, $\Delta\delta_{AB}$ = 0.02, J_{AB} = 8.0 Hz), 6.82 (s, 4 H), 2.31 (s, 6 H), 1.99 (s, 12 H).

Compound **5**.[12] 1,3,5-Tribromobenzene (**4**) (2.00 g, 6.35 mmol) was dissolved in dry Et_2O (30 mL) under N_2 and cooled to −78 °C. *n*-BuLi in hexane (2.54 mL, 6.35 mmol) was added dropwise, and the reaction mixture was stirred at −78 °C for 2 h. Dimesitylboron fluoride (**2**) (1.70 g, 6.35 mmol) was added, and the suspension was stirred at room temperature for 1 h. Then, the solution was diluted with hexane (100 mL), washed with water, and dried over Na_2SO_4. Chromatography on a silica gel column with pentane gave the pure product as a white solid (2.12 g, 4.38 mmol, 69%). ^{1}H NMR (400 MHz, $CDCl_3$): δ [ppm] 7.76 (t, J = 1.9 Hz, 1 H), 7.51 (d, J = 1.9 Hz, 2 H), 6.82 (s, 4 H), 2.31 (s, 6 H), 1.97 (s, 12 H).

Compound **6**.[13] Compound **5** (2.10 g, 4.34 mmol)[12] was reacted with *n*-BuLi in hexane (1.74 mL, 4.34 mmol) and dimesitylboron fluoride (**2**) (1.16 g, 4.34 mmol) as described above for compound **5**. Chromatography on silica gel with pentane afforded the product as a white solid (1.96 g, 2.99 mmol, 69%). ^{1}H NMR (400 MHz, $CDCl_3$): δ [ppm] 7.65 (d, J = 1.1 Hz, 2 H), 7.38 (t, J = 1.1 Hz, 1 H), 6.75 (s, 8 H), 2.28 (s, 12 H), 1.94 (s, 24 H).

N-ph-B. Compound **3** (0.20 g, 0.51 mmol),[11] dianisylamine (**7**) (0.11 g, 0.47 mmol), NaO^{t}Bu (0.82 g, 8.5 mmol), $Pd(dba)_2$ (23 mg, 0.04 mmol), and $(HP^tBu_3)BF_4$ (8.3 mg, 0.04 mmol) were dissolved in dry deoxygenated toluene (15 mL) under N_2. The mixture was reacted at 120 °C for 2 h. Brine (100 mL) was added to the cooled solution, and the aqueous phase was extracted with CH_2Cl_2 (3 × 50 mL). The solvents were evaporated after drying over Na_2SO_4, and the crude product was purified by column chromatography on silica gel. The eluent was an 18:1 (v:v) mixture of pentane and EtOAc. The pure product was obtained as a bright yellow solid (0.24 g, 0.43 mmol, 92%). ^{1}H NMR (250 MHz, DMSO-d_6): δ [ppm] 7.21−7.10 (m, 6 H), 6.99−6.91 (m, 4 H), 6.77 (s, 4 H), 6.61 (d, J = 8.7 Hz, 2 H), 3.74 (s, 6 H), 2.22 (s, 6 H), 1.97 (s, 12 H). ^{13}C NMR (100 MHz, DMSO-d_6): δ [ppm] 156.7, 152.1, 141.4, 139.7, 138.5, 138.2, 137.2, 134.3, 128.1, 127.9, 115.3, 115.0, 55.2, 23.0, 20.7. HRMS (ESI TOF) m/z: $[M]^+$ Calcd for $C_{38}H_{40}NO_2B$ 553.3153; Found 553.3147. Anal. Calcd for $C_{38}H_{40}NO_2B$: C, 82.45; H, 7.28; N, 2.53. Found: 82.05; H, 7.29; N, 2.40.

N_3-ph-B. Compound **3** (72 mg, 0.18 mmol),[11] oligotriarylamine **8** (100 mg, 0.16 mmol),[10c] NaO^{t}Bu (308 mg, 3.2 mmol), $Pd(dba)_2$ (12 mg, 0.02 mmol), and $(HP^tBu_3)BF_4$ (4.6 mg, 0.02 mmol) were dissolved in dry and deoxygenated toluene (100 mL) under N_2. The mixture was refluxed for 1.25 h and then cooled to room temperature. Brine (100 mL) was added, and the aqueous phase was extracted with CH_2Cl_2 (3 × 50 mL). The combined organic phases were dried over Na_2SO_4 and evaporated. Chromatography on a silica gel column with a 1:1 (v:v) mixture of pentane and CH_2Cl_2 followed by recrystallization from acetone afforded the pure product as a bright yellow solid (117 mg, 0.12 mmol, 77%). ^{1}H NMR (400 MHz, acetone-d_6): δ [ppm] 7.31−7.25 (m, 2 H), 7.11−7.02 (m, 12 H), 6.93−6.84 (m, 12 H), 6.82−6.76 (m, 6 H), 3.78 (s, 12 H), 2.25 (s, 6 H), 2.04 (s, 12 H). ^{13}C NMR (100 MHz, C_6D_6): δ [ppm] 156.2, 152.5, 146.1, 142.4, 141.2, 140.7, 139.5, 137.6, 136.2, 128.4, 127.6, 126.5, 125.7, 121.9, 117.1, 114.9, 54.7, 23.6, 21.0. HRMS (ESI TOF) m/z: $[M]^+$ Calcd for $C_{64}H_{62}N_3O_4B$ 947.4838; Found 947.4834. Anal. Calcd for $C_{64}H_{62}N_3O_4B{\cdot}0.5H_2O$: C, 80.32; H, 6.64; N, 4.39. Found: 80.36; H, 6.81; N, 4.46. Water is also detected in the ^{1}H NMR spectrum; see the Supporting Information.

N_3-ph-B_2. Compound **6** (118 mg, 0.18 mmol),[13] oligotriarylamine **8** (100 mg, 0.16 mmol),[10c] NaO^{t}Bu (308 mg, 3.2 mmol), $Pd(dba)_2$ (12 mg, 0.02 mmol), and $(HP^tBu_3)BF_4$ (4.6 mg, 0.02 mmol) were dissolved in dry deoxygenated toluene (10 mL) under N_2. The mixture was refluxed for 1 h and then cooled to room temperature. Brine (100 mL) was added, and after phase separation, the aqueous layer was extracted with CH_2Cl_2 (3 × 50 mL). After drying over Na_2SO_4 and evaporation of the solvents, the crude product was purified on a silica gel column. First, the eluent was a 1:1 (v:v) mixture of pentane and CH_2Cl_2, and then, pure CH_2Cl_2 was used. The pure product crystallized when dropping a concentrated CH_2Cl_2 solution into methanol (120 mg, 0.10 mmol, 63%). ^{1}H NMR (400 MHz, acetone-d_6): δ [ppm] 7.27 (d, J = 1.1 Hz, 2 H), 7.22 (t, J = 1.1 Hz, 1 H), 6.97−6.92 (m, 8 H), 6.90−6.84 (m, 12 H), 6.79−6.74 (m, 12 H), 3.79 (s, 12 H), 2.22 (s, 12 H), 1.98 (s, 24 H). ^{13}C NMR (100 MHz, acetone-d_6): δ [ppm] 156.8, 145.1, 142.8, 142.3, 141.4, 139.7, 138.4, 136.8, 134.2, 129.2, 127.8, 126.7, 125.7, 123.6, 120.1, 115.6, 55.9, 23.8, 21.6. HRMS (ESI TOF) m/z: $[M]^+$ Calcd for $C_{82}H_{83}N_3O_4B_2$ 1195.6588; Found 1195.6576. Anal. Calcd for $C_{82}H_{83}N_3O_4B_2{\cdot}0.5H_2O$: C, 81.72; H, 7.02; N, 3.49. Found: 81.83; H, 6.95; N, 3.44. Water is also detected in the ^{1}H NMR spectrum; see the Supporting Information.

Compound **11**.[14] 4-Bromo-1-iodobenzene (**9**) (2.00 g, 7.06 mmol) and trimethylsilyl acetylene (**10**) (1.10 mL, 7.78 mmol) were dissolved

DOI: 10.1021/acs.joc.5b00416
J. Org. Chem. 2015, 80, 4097−4107

in dry Et_3N (30 mL) under N_2. $PdCl_2(PPh_3)_2$ (98 mg, 0.14 mmol) and CuI (53 mg, 0.28 mmol) were added, and the reaction mixture was heated to 100 °C for 30 min. After cooling to room temperature, saturated aqueous NH_4Cl solution (100 mL) was added and the product was extracted with CH_2Cl_2 (3 × 50 mL). The organic phases were dried over Na_2SO_4 and evaporated. Chromatography on a silica gel column with pentane gave a white solid (1.80 g, 7.11 mmol, ~100%). ^{1}H NMR (400 MHz, $CDCl_3$): δ [ppm] 7.45−7.41 (m, 2 H), 7.33−7.30 (m, 2 H), 0.25 (s, 9 H).

Compound **12**.[15] Compound **11** (1.00 g, 4.0 mmol),[14] dianisylamine (**7**) (725 mg, 3.2 mmol), NaO^{t}Bu (6.3 mg, 65.6 mmol), $Pd(dba)_2$ (190 mg, 0.3 mmol), and P^{t}Bu$_3$ (0.98 mL, 0.3 mmol) were dissolved in dry deoxygenated toluene (60 mL) under N_2. The mixture was refluxed for 30 h, and after cooling to room temperature, brine (100 mL) was added. After phase separation, the aqueous layer was extracted with CH_2Cl_2 (3 × 50 mL), and the combined organic phases were dried over Na_2SO_4. Column chromatography on silica gel with a 1:3 (v:v) mixture of pentane and CH_2Cl_2 afforded the pure product as a yellow solid (810 mg, 2.0 mmol, 64%). ^{1}H NMR (250 MHz, acetone-d_6): δ [ppm] 7.27−7.19 (m, 2 H), 7.12−7.05 (m, 4 H), 6.97−6.89 (m, 4 H), 6.76−6.68 (m, 2 H), 3.80 (s, 6 H), 0.2 (s, 9 H).

Compound **13**. Compound **11** (150 mg, 0.59 mmol), oligotriarylamine **8** (308 mg, 0.49 mmol),[10c] NaO^{t}Bu (942 mg, 9.80 mmol), $Pd(dba)_2$ (28 mg, 0.05 mmol), and (HP^{t}Bu$_3$)BF$_4$ (14 mg, 0.05 mmol) were dissolved in dry and deoxygenated toluene (15 mL). The mixture was refluxed under N_2 for 20 h. Brine (100 mL) was added to the cooled mixture, and the aqueous phase was extracted with CH_2Cl_2 (3 × 50 mL). After drying over Na_2SO_4 and evaporation of the solvents, the crude product was purified by column chromatography on silica gel using CH_2Cl_2 as the eluent. The pure product was obtained as a yellow oil which solidified over time (290 mg, 0.36 mmol, 74%). ^{1}H NMR (400 MHz, acetone-d_6): δ [ppm] 7.25−7.23 (m, 2 H), 7.08−7.06 (m, 8 H), 6.99−6.97 (m, 4 H), 6.90−6.82 (m, 14 H), 3.78 (s, 12 H), 0.19 (s, 9 H).

Compound **14**.[15] Compound **12** (0.80 g, 2.0 mmol) was dissolved in THF (40 mL) under N_2, and TBAF solution in methanol (18.0 mL, 5.4 mmol) was added dropwise. The reaction mixture was stirred at room temperature for 1 h, and then, the solvents were evaporated. The solid residue was taken up in EtOAc and washed with water (3 × 100 mL). After drying over Na_2SO_4 and evaporating the solvent, the pure product was obtained as a yellow solid (0.65 g, 2.0 mmol, 99%). ^{1}H NMR (250 MHz, $CDCl_3$): δ [ppm] 7.30−7.23 (m, 2 H), 7.11−7.01 (m, 4 H), 6.89−6.76 (m, 6 H), 3.80 (s, 6 H).

Compound **15**. Compound **13** (300 mg, 0.38 mmol) was dissolved in dry THF (10 mL) under N_2. TBAF solution in THF (1.40 mL, 0.38 mmol) was added dropwise, and the reaction mixture was stirred at room temperature for 1.5 h. After removal of THF, the solid residue was taken up in EtOAc (100 mL) and washed with water. The organic phases were dried over Na_2SO_4 and evaporated to dryness. This afforded the pure product as a yellow solid (250 mg, 0.35 mmol, 91%). ^{1}H NMR (400 MHz, C_6D_6): δ [ppm] 7.38−7.36 (m, 2 H), 7.12−7.07 (m, 8 H), 7.05−6.97 (m, 10 H), 6.73−6.68 (m, 8 H), 3.29 (s, 12 H), 2.76 (s, 1 H).

N-phCC-B.[9b] Compound **3** (270 mg, 0.67 mmol) and compound **14** (200 mg, 0.61 mmol) were suspended in dry Et_3N (15 mL) under N_2. CuI (4.5 mg, 0.02 mmol) and $PdCl_2(PPh_3)_2$ (8.4 mg, 0.01 mmol) were added, and the reaction mixture was refluxed for 30 h. After cooling to room temperature, saturated aqueous NH_4Cl solution (100 mL) was added, and the aqueous phase was extracted with CH_2Cl_2 (3 × 50 mL). After drying over Na_2SO_4 and evaporation of the solvents, the crude product was purified by chromatography on silica gel using an 18:1 (v:v) mixture of pentane and EtOAc as the eluent. Subsequent recrystallization by dropping a concentrated CH_2Cl_2 solution into methanol afforded the pure product as a yellow solid (172 mg, 0.26 mmol, 43%). ^{1}H NMR (250 MHz, acetone-d_6): δ [ppm] 7.49 (ABq, 4 H, $\Delta\delta_{AB}$ = 0.04, J_{AB} = 8.8 Hz), 7.38−7.32 (m, 2 H), 7.16−7.09 (m, 4 H), 6.99−6.91 (m, 4 H), 6.85 (s, 4 H), 6.81−6.75 (m, 2 H), 3.81 (s, 6 H), 2.29 (s, 6 H), 2.00 (s, 12 H). ^{13}C NMR (100 MHz, acetone-d_6): δ [ppm] 158.9, 151.5, 147.3, 143.4, 142.5, 141.6, 140.8, 138.0, 134.5, 132.7, 130.2, 129.5, 129.4, 120.0, 116.9, 114.8, 94.7, 90.1, 56.9, 24.8, 22.4. HRMS (ESI TOF) m/z: [M]$^+$ Calcd for $C_{46}H_{44}NO_2B$ 653.3467; Found 653.3456. Anal. Calcd for $C_{46}H_{44}NO_2B{\cdot}0.5H_2O$: C, 83.37; H, 6.84; N, 2.11. Found: 83.74; H, 6.83; N, 2.20. Water is also detected in the ^{1}H NMR spectrum; see the Supporting Information.

N_3-phCC-B. Compound **15** (217 mg, 0.30 mmol) and compound **3** (100 mg, 0.25 mmol) were dissolved in dry Et_3N (10 mL) under a N_2 atmosphere. $PdCl_2(PPh_3)_2$ (3.5 mg, 0.005 mmol) and CuI (1.9 mg, 0.01 mmol) were added, and the reaction mixture was refluxed overnight. After cooling to room temperature, saturated aqueous NH_4Cl solution was added, and the product was extracted with CH_2Cl_2 (3 × 50 mL). The combined organic phases were dried over Na_2SO_4 and evaporated. Chromatography on a silica gel column with a 1:2 (v:v) mixture of pentane and CH_2Cl_2 afforded the product as an orange oil (110 mg, 0.11 mmol, 42%). When drops of a concentrated solution of this oil in CH_2Cl_2 were added to water, an orange solid was obtained. ^{1}H NMR (400 MHz, acetone-d_6): δ [ppm] 7.48 (ABq, 4 H, $\Delta\delta_{AB}$ = 0.02, J_{AB} = 8.0 Hz), 7.37−7.33 (m, 2 H), 7.07−7.00 (m, 12 H), 6.91−6.84 (m, 18 H), 3.77 (s, 12 H), 2.28 (s, 6 H), 2.00 (s, 12 H). ^{13}C NMR (100 MHz, acetone-d_6): δ [ppm] 157.2, 150.2, 146.7, 146.4, 142.5, 141.9, 140.4, 139.8, 139.1, 137.1, 129.3, 127.9, 127.5, 122.4, 119.8, 115.7, 114.1, 93.8, 89.3, 55.9, 23.9, 21.4. HRMS (ESI TOF) m/z: [M]$^+$ Calcd for $C_{72}H_{66}N_3O_4B$ 1047.5152; Found 1047.5127. Anal. Calcd for $C_{72}H_{66}N_3O_4B$: C, 82.51; H, 6.35; N, 4.01. Found: 82.45; H, 6.65; N, 3.80.

N_3-phCC-B_2. Compound **15** (180 mg, 0.25 mmol) and compound **6** (195 mg, 0.29 mmol)[13] were suspended in dry Et_3N (10 mL) under N_2. $PdCl_2(PPh_3)_2$ (3.5 mg, 0.005 mmol) and CuI (1.9 mg, 0.01 mmol) were added, and the mixture was reacted at reflux overnight. After cooling to room temperature, saturated aqueous NH_4Cl solution (100 mL) was added and the product was extracted with CH_2Cl_2 (3 × 50 mL). The combined organic phases were dried over Na_2SO_4 and evaporated. Column chromatography on silica gel with a 1:2 (v:v) mixture of pentane and CH_2Cl_2 gave a yellow oil. When drops of a concentrated solution of this oil in CH_2Cl_2 were added to methanol, the product was obtained as an orange solid (110 mg, 0.09 mmol, 34%). ^{1}H NMR (400 MHz, acetone-d_6): δ [ppm] 7.66 (d, J = 1.3 Hz, 2 H), 7.54 (t, J = 1.3 Hz, 1 H), 7.25 (d, J = 8.7 Hz, 2 H), 7.07−7.01 (m, 8 H), 6.98 (d, J = 8.7 Hz, 4 H), 6.92−6.68 (m, 8 H), 6.86−6.81 (m, 6 H), 6.79 (s, 8 H), 3.77 (s, 12 H), 2.24 (s, 12 H), 1.97 (s, 24 H). ^{13}C NMR (100 MHz, acetone-d_6): δ [ppm] 157.2, 149.9, 148.0, 146.7, 142.5, 142.2, 141.9, 141.5, 140.5, 140.2, 133.4, 129.3, 127.7, 127.4, 124.8, 122.4, 119.8, 115.8, 115.2, 114.2, 91.6, 88.9, 55.9, 23.9, 21.5. HRMS (ESI TOF) m/z: [M]$^+$ Calcd for $C_{90}H_{87}N_3O_4B_2$ 1295.6902; Found 1295.6878. Anal. Calcd for $C_{90}H_{87}N_3O_4B_2{\cdot}0.5H_2O$: C, 82.81; H, 6.80; N, 3.22. Found: 82.64; H, 6.74; N, 2.94. Water is also detected in the ^{1}H NMR spectrum; see the Supporting Information.

NMR spectroscopy, ESI-HRMS, elemental analysis, cyclic voltammetry, optical absorption, and luminescence spectroscopy occurred using the same equipment as described in detail in a recent publication.[10c] Fluorescence lifetime measurements were performed using a commercial fluorescence lifetime spectrometer. Absolute photoluminescence quantum yields were measured on a commercial absolute photoluminescence quantum yield measurement system.

■ ASSOCIATED CONTENT

Supporting Information

^{1}H and ^{1}H/^{13}C-HMBC NMR spectra, ESI-HRMS spectra, and additional electrochemical and optical spectroscopic data. This material is available free of charge via the Internet at http://pubs.acs.org.

■ AUTHOR INFORMATION

Corresponding Author

*E-mail: oliver.wenger@unibas.ch

Notes

The authors declare no competing financial interest.

DOI: 10.1021/acs.joc.5b00416
J. Org. Chem. 2015, 80, 4097−4107

■ ACKNOWLEDGMENTS

This work was supported by the Swiss National Science Foundation through grant number 200021_146231/1 and by the Deutsche Forschungsgemeinschaft through grant number WE4815/3-1.

■ REFERENCES

(1) Hagfeldt, A.; Boschloo, G.; Sun, L. C.; Kloo, L.; Pettersson, H. *Chem. Rev.* **2010**, *110*, 6595.
(2) (a) Marder, S. R.; Cheng, L. T.; Tiemann, B. G.; Friedli, A. C.; Blanchard-Desce, M.; Perry, J. W.; Skindhoj, J. *Science* **1994**, *263*, 511. (b) Kim, H. M.; Cho, B. R. *Acc. Chem. Res.* **2009**, *42*, 863.
(3) Hide, F.; DiazGarcia, M. A.; Schwartz, B. J.; Heeger, A. J. *Acc. Chem. Res.* **1997**, *30*, 430.
(4) Glasbeek, M.; Zhang, H. *Chem. Rev.* **2004**, *104*, 1929.
(5) (a) Entwistle, C. D.; Marder, T. B. *Angew. Chem., Int. Ed.* **2002**, *41*, 2927. (b) Elbing, M.; Bazan, G. C. *Angew. Chem., Int. Ed.* **2008**, *47*, 834. (c) Yamaguchi, S.; Wakamiya, A. *Pure Appl. Chem.* **2006**, *78*, 1413. (d) Jäkle, F. *Chem. Rev.* **2010**, *110*, 3985. (e) Lorbach, A.; Bolte, M.; Li, H. Y.; Lerner, H. W.; Holthausen, M. C.; Jäkle, F.; Wagner, M. *Angew. Chem., Int. Ed.* **2009**, *48*, 4584.
(6) (a) Wade, C. R.; Broomsgrove, A. E. J.; Aldridge, S.; Gabbaï, F. P. *Chem. Rev.* **2010**, *110*, 3958. (b) Broomsgrove, A. E. J.; Addy, D. A.; Bresner, C.; Fallis, I. A.; Thompson, A. L.; Aldridge, S. *Chem.—Eur. J.* **2008**, *14*, 7525. (c) Hudnall, T. W.; Chiu, C. W.; Gabbaï, F. P. *Acc. Chem. Res.* **2009**, *42*, 388. (d) Yamaguchi, S.; Akiyama, S.; Tamao, K. *J. Am. Chem. Soc.* **2000**, *122*, 6335. (e) Liu, X. Y.; Bai, D. R.; Wang, S. N. *Angew. Chem., Int. Ed.* **2006**, *45*, 5475. (f) Sun, Y.; Ross, N.; Zhao, S. B.; Huszarik, K.; Jia, W. L.; Wang, R. Y.; Macartney, D.; Wang, S. N. *J. Am. Chem. Soc.* **2007**, *129*, 7510.
(7) Yamaguchi, S.; Shirasaka, T.; Akiyama, S.; Tamao, K. *J. Am. Chem. Soc.* **2002**, *124*, 8816.
(8) (a) Zhao, C. H.; Wakamiya, A.; Inukai, Y.; Yamaguchi, S. *J. Am. Chem. Soc.* **2006**, *128*, 15934. (b) Zhou, G.; Baumgarten, M.; Müllen, K. *J. Am. Chem. Soc.* **2008**, *130*, 12477. (c) Hudson, Z. M.; Wang, S. N. *Acc. Chem. Res.* **2009**, *42*, 1584. (d) Schmidt, H. C.; Reuter, L. G.; Hamacek, J.; Wenger, O. S. *J. Org. Chem.* **2011**, *76*, 9081. (e) Chen, P. K.; Jäkle, F. *J. Am. Chem. Soc.* **2011**, *133*, 20142. (f) Mengel, A. K. C.; He, B.; Wenger, O. S. *J. Org. Chem.* **2012**, *77*, 6545. (g) Entwistle, C. D.; Marder, T. B. *Chem. Mater.* **2004**, *16*, 4574. (h) Pron, A.; Zhou, G.; Norouzi-Arasi, H.; Baumgarten, M.; Müllen, K. *Org. Lett.* **2009**, *11*, 3550.
(9) (a) Chen, P. K.; Lalancette, R. A.; Jäkle, F. *Angew. Chem., Int. Ed.* **2012**, *51*, 7994. (b) Steeger, M.; Lambert, C. *Chem.—Eur. J.* **2012**, *18*, 11937.
(10) (a) Hirao, Y.; Ito, A.; Tanaka, K. *J. Phys. Chem. A* **2007**, *111*, 2951. (b) Karlsson, S.; Boixel, J.; Pellegrin, Y.; Blart, E.; Becker, H. C.; Odobel, F.; Hammarström, L. *J. Am. Chem. Soc.* **2010**, *132*, 17977. (c) Bonn, A. G.; Neuburger, M.; Wenger, O. S. *Inorg. Chem.* **2014**, *53*, 11075.
(11) Xu, X. F.; Ye, S. H.; He, B. R.; Chen, B.; Xiang, J. Y.; Zhou, J.; Lu, P.; Zhao, Z. J.; Qiu, H. Y. *Dyes Pigm.* **2014**, *101*, 136.
(12) Rao, Y.-L.; Schoenmakers, D.; Chang, Y.-L.; Lu, J.-S.; Lu, Z.-H.; Kang, Y.; Wang, S. *Chem.—Eur. J.* **2012**, *18*, 11306.
(13) Cunningham, A. F.; Kunz, M.; Kura, H. Photoinitiators comprising boranes and electron donors. Eur. Pat. Appl. 2002, EP 1203999 A2 20020508.
(14) Florian, A.; Mayoral, M. J.; Stepanenko, V.; Fernandez, G. *Chem.—Eur. J.* **2012**, *18*, 14957.
(15) (a) Zieschang, F.; Schreck, M. H.; Schmiedel, A.; Holzapfel, M.; Klein, J. H.; Walter, C.; Engels, B.; Lambert, C. *J. Phys. Chem. C* **2014**, *118*, 27698. (b) Lambert, C.; Nöll, G.; Schmälzlin, E.; Meerholz, K.; Bräuchle, C. *Chem.—Eur. J.* **1998**, *4*, 2129.
(16) (a) Sreenath, K.; Thomas, T. G.; Gopidas, K. R. *Org. Lett.* **2011**, *13*, 1134. (b) Kaim, W.; Schulz, A. *Angew. Chem., Int. Ed.* **1984**, *23*, 615.
(17) (a) Stahl, R.; Lambert, C.; Kaiser, C.; Wortmann, R.; Jakober, R. *Chem.—Eur. J.* **2006**, *12*, 2358. (b) Bai, D. R.; Liu, X. Y.; Wang, S. I. *Chem.—Eur. J.* **2007**, *13*, 5713.
(18) Reichardt, C. *Chem. Rev.* **1994**, *94*, 2319.
(19) (a) Lippert, E. *Z. Naturforsch., A* **1955**, *10*, 541. (b) Mataga, N.; Kaifu, Y.; Koizumi, M. *Bull. Chem. Soc. Jpn.* **1955**, *28*, 690.
(20) Onsager, L. *J. Am. Chem. Soc.* **1936**, *58*, 1486.
(21) Suppan, P. *Chem. Phys. Lett.* **1983**, *94*, 272.
(22) Caspar, J. V.; Meyer, T. J. *J. Phys. Chem.* **1983**, *87*, 952.
(23) Zhang, Z.; Edkins, R. M.; Nitsch, J.; Fucke, K.; Steffen, A.; Longobardi, L. E.; Stephan, D. W.; Lambert, C.; Marder, T. B. *Chem. Sci.* **2015**, *6*, 308.

DOI: 10.1021/acs.joc.5b00416
J. Org. Chem. 2015, 80, 4097−4107